NATIONAL AERONAUTICS AND SPACE ADMINISTRATION

Technical Report 32-1426

Results of the 1968 Balloon Flight Solar Cell Standardization Program

Richard F. Greenwood

JET PROPULSION LABORATORY
CALIFORNIA INSTITUTE OF TECHNOLOGY
PASADENA, CALIFORNIA

December 1, 1969

NATIONAL AERONAUTICS AND SPACE ADMINISTRATION

Technical Report 32-1426

Results of the 1968 Balloon Flight Solar Cell Standardization Program

Richard F. Greenwood

JET PROPULSION LABORATORY
CALIFORNIA INSTITUTE OF TECHNOLOGY
PASADENA, CALIFORNIA

December 1, 1969

Prepared Under Contract No. NAS 7-100
National Aeronautics and Space Administration

Preface

The work described in this report was performed by the Guidance and Control Division of the Jet Propulsion Laboratory.

Contents

Tables

Figures

Contents (contd)

Figures (contd)

Abstract

The difficulty in predicting the space power output of solar cell arrays by means of terrestrial measurements has been minimized by the use of high-altitude balloons for solar cell calibration. A cooperative effort between the Jet Propulsion Laboratory and other NASA and government agencies has made space-calibrated standard solar cells available for a variety of space projects. The use of high-altitude balloons has not only provided standard solar cells but has also furnished a means of lifting radiometers above the earth's atmosphere to measure the solar constant.

Results of the 1968 Balloon Flight Solar Cell Standardization Program

I. Introduction

Solar cells are the main source of electrical power for unmanned spacecraft. The power output from solar cells operating in space must be accurately predicted from terrestrial sunlight measurements. However, terrestrial sunlight is unlike space sunlight in both intensity and spectral content, making accurate extrapolation of terrestrial measurements by conventional methods difficult. In recent years, this difficulty has been reduced by the use of standard solar cells whose space short-circuit current is known. Since the short-circuit current of a solar cell is directly proportional to intensity over a sun distance of approximately 0.5 to 5.0 AU, a properly calibrated solar cell can serve as an intensity reference.

The purpose of the solar cell standardization program conducted at the Jet Propulsion Laboratory (JPL) is to provide standard solar cells applicable to current solar cell and solar array testing programs. Standard solar cells are calibrated on high-altitude balloon flights which ascend above 97% of the earth's atmosphere. This report discusses the results of three balloon flights conducted during the months of July and August 1968 in the vicinity of Minneapolis, Minnesota.

II. Balloon Flight System

The main components of the balloon flight system are a sun tracker, a helium-filled balloon, a telemetry system, and a battery power supply, as shown in Fig. 1. The sun tracker is mounted on the balloon apex, which is the most stable position of the balloon system. The telemetry transmitter and battery power supply, along with several instruments for measuring altitude, are suspended beneath the balloon. An electrical cable, incorporated into the balloon during manufacture, connects the top and bottom payloads. A parachute is provided in the event of balloon failure.

The solar tracker is used to position the solar cell payload toward the sun, independent of balloon movements. The tracker is capable of movement in both elevation and azimuth to maintain an "on-sun" condition within ± 2 deg. A reflection shield attached to the solar tracker is used to prevent unwanted reflected light from reaching the solar cell payload.

Improvements in the solar tracker are periodically being made. Prior to the 1968 balloon flights, the tracker was modified to provide for a larger solar cell payload

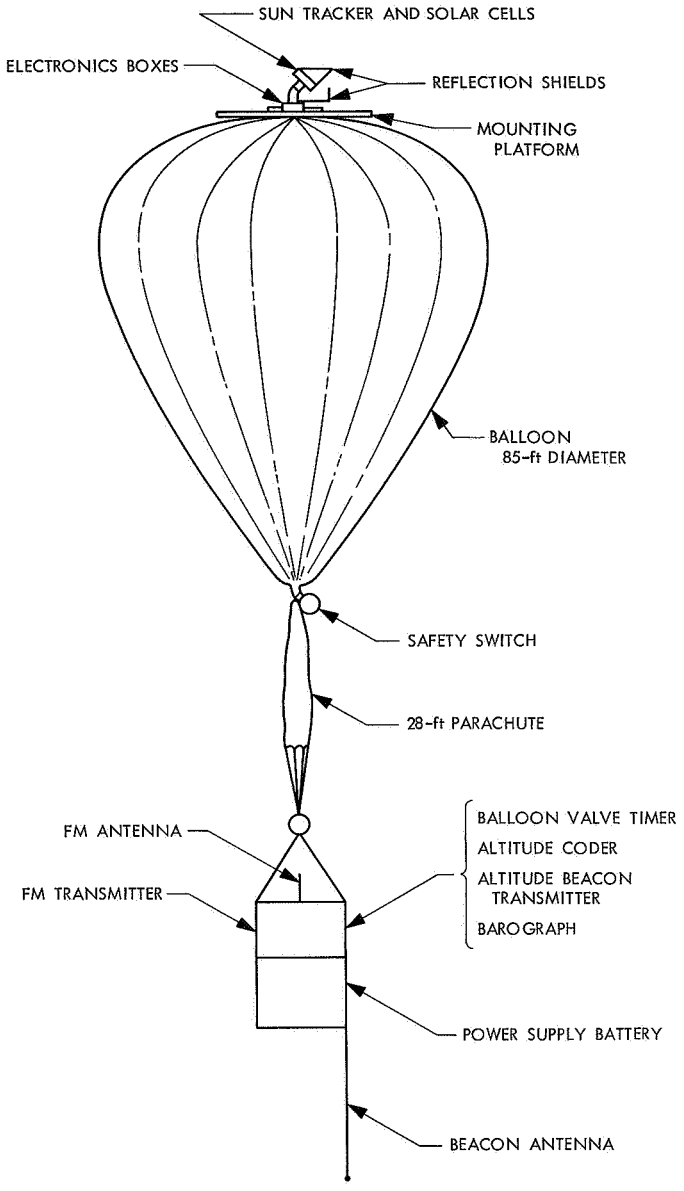

Fig. 1. Balloon flight system

(Fig. 2). A 36-position stepping switch replaced the former 24-position stepping switch, thus adding a 12-data-channel capability increase. At the same time, the solar cell payload mounting area was increased to provide for the 12 additional solar cells.

One of the trackers was further modified to provide special mounting for the radiometer and filter wheel experiment (described later). This modification was performed by the contractor, Litton Systems, Inc., after the radiometer experiment was delivered by JPL. Design and fabrication were completed in only 5 days.

The tracker and associated electronics boxes are mounted on a plywood disk 6 ft (1.83 m) in diameter, which, in turn, is bolted to the balloon top end fitting. The plywood disk permits the tracker to "float" on top of the helium bubble. Total weight of the upper payload is approximately 50 lb (22.68 kg).

The balloon used for the normal flights of 80,000 ft (24,384 m) altitude is 85 ft (25.91 m) in diameter when fully inflated and has a volume of approximately 243,000 ft^3 (6,882 m^3). The balloon is fabricated from 1.5-mil polyethylene material designed especially for balloon use. During inflation, the helium is confined to the upper portion of the balloon by a launching mechanism to reduce problems associated with surface winds. The body of the balloon, protected by a polyethylene sheath, extends along the ground from the balloon launcher to a launch truck. The lower payload, containing the battery power supply and telemetry transmitter, is attached to the launch truck by an explosive bolt.

The balloon is launched by releasing the upper portion of the balloon held by the launching mechanism. As the balloon rises, the launch truck is driven downwind to position the lower payload directly under the balloon body. At this point, the explosive bolt is fired by push-button controls within the launch truck and the balloon is free from ground constraint.

Several functions are performed by pressure switches and timing devices as the flight progresses. At a 5,000-ft (1524-m) altitude, a pressure switch activates a circuit deploying a long dipole beacon antenna. At 20,000 ft (6096 m), a second pressure switch activates the sun tracker, permitting it to lock on the sun. At the completion of the float period, a preset timer opens a valve in the side of the balloon, allowing helium to escape at a controlled rate and causing the balloon and its associated equipment to descend to the earth.

The heart of the telemetry system is the voltage-controlled oscillator. Solar cell voltages, interspersed with reference voltages and thermistor circuit voltages, are fed into the voltage-controlled oscillator, converted to frequencies, and transmitted to a ground station by a 5-W FM transmitter. At the ground station, telemetry data are recorded on printed paper tape in digital form and also displayed in analog form on a strip chart recorder. The solar cell data are then transferred from the printed tape to punch cards compatible with a JPL computer program.

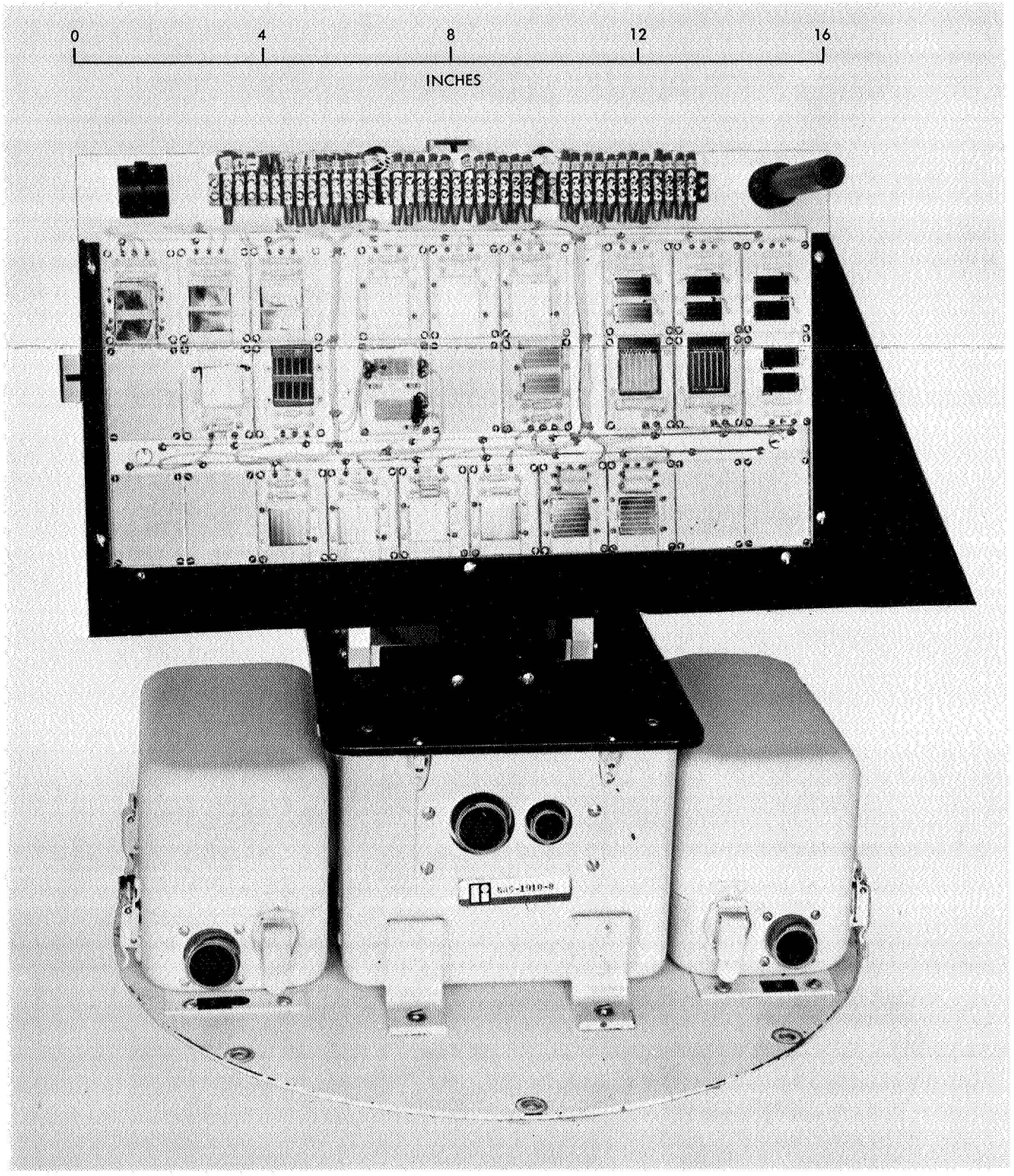

Fig. 2. Modified tracker for balloon flights 1 and 2

The battery power supply provides adequate power for a normal flight while keeping weight to a minimum. Aircraft-type lead–acid batteries are used to provide main power for the telemetry transmitter, the stepping switch, and several temperature-controlling heaters. The solar tracker is electrically isolated from the main batteries and is powered by a separate alkaline-type dry battery. The total weight of the battery power supply is 78 lb (35.38 kg).

III. Balloon Flight Payloads

Solar cells are manufactured in many types and configurations. Several of the cell types and configurations, mounted in standard modules, were supplied by various NASA and government agencies in a cooperative effort with JPL to provide calibrated standard solar cells at a minimum expense.

The NASA Goddard Space Flight Center sponsored standard solar cells for use with the solar panels on the Orbiting Astronomical Observatory (OAO) spacecraft. Heliotek[1] 1 × 2-cm *n–p* cells are used on the panels, and representative cells were supplied in modular form for balloon flight calibration. The Goddard Space Flight Center also sponsored silicon 2 × 2-cm *n–p* solar cells from two West German manufacturers, Allgemeine Elektricitäts-Gesellschaft (AEG) and Siemens Aktiengesellschaft, intended for use as standards with the German Research Satellite Program.

The United States Air Force Aeropropulsion Laboratory furnished developmental solar cells of the three types, as follows:

(1) 2 × 2-cm *n–p* ion-implanted silicon.

(2) 1 × 2-cm thin-film cadmium sulfide (CdS).

(3) 1 × 2-cm thin-film cadmium telluride (CdTe).

These standard cells are used to calibrate solar simulators for testing similar developmental solar cells.

The NASA Langley Research Center participated in the cooperative effort by supplying four 1 × 2-cm silicon cells for use in calibrating solar simulators.

Several solar cell modules were fabricated by JPL for use as standards with the *Mariner Mars 1969* and *Mariner Mars 1971* flight programs. The solar cells are 2 × 2-cm *n–p* silicon cells manufactured by Heliotek and covered with a 0.41μm cut-on quartz filter (Fig. 3). Both the solar cells and the 20-mil-thick quartz filters are representative of the devices used on the solar panels.

In addition to the cells described above, several cells were covered with optical bandpass filters, thus permitting only selected wavelengths of sunlight to reach the solar cells. Solar cells and bandpass filter combinations are used to evaluate the spectral content of solar simulators. One such set of four solar cell–filter combinations was submitted for calibration by the Applied Physics Laboratory of the Johns Hopkins University. The Jet Propulsion Laboratory provided a set of three solar cell–filter combinations intended to aid in evaluating bandpass filters for use on the spacecraft solar arrays of possible near-sun missions (Fig. 4).

A special three-cell module having different filters on each cell was fabricated to provide a combination spectral and intensity monitor for use in conjunction with JPL's Spectrolab[1] X-25L (Spectrosun) solar simulator (Fig. 5). The two smaller cells are used to monitor the red-to-blue spectral ratio of the light source, while the 1 × 2-cm cell is used as an aid in setting and monitoring the light intensity. This standard will be mounted in a test chamber so that continuous monitoring of the light source is permitted during cell testing, thus permitting uninterrupted, long-duration tests.

Besides the solar cell calibration, a unique experiment was devised, consisting of two radiometers designed and built by JPL, four solar cells, and a filter wheel. The purpose of the experiment was to measure the solar constant more accurately, as well as to gather data in selected wavelength bands. The JPL Instrumentation Section and the Spacecraft Power Section cooperated in this joint effort.

The radiometers (enclosed, standard cavity active radiometers) are designed to measure total sun radiation. These radiometers are highly accurate; a similar basic design is described in Ref. 1.

Four different solar cells were selected, each cell having a slightly different spectral response. The cells were mounted in standard modules and positioned under the filter wheel adjacent to the radiometers.

[1]A division of Textron, Inc., Sylmar, Calif.

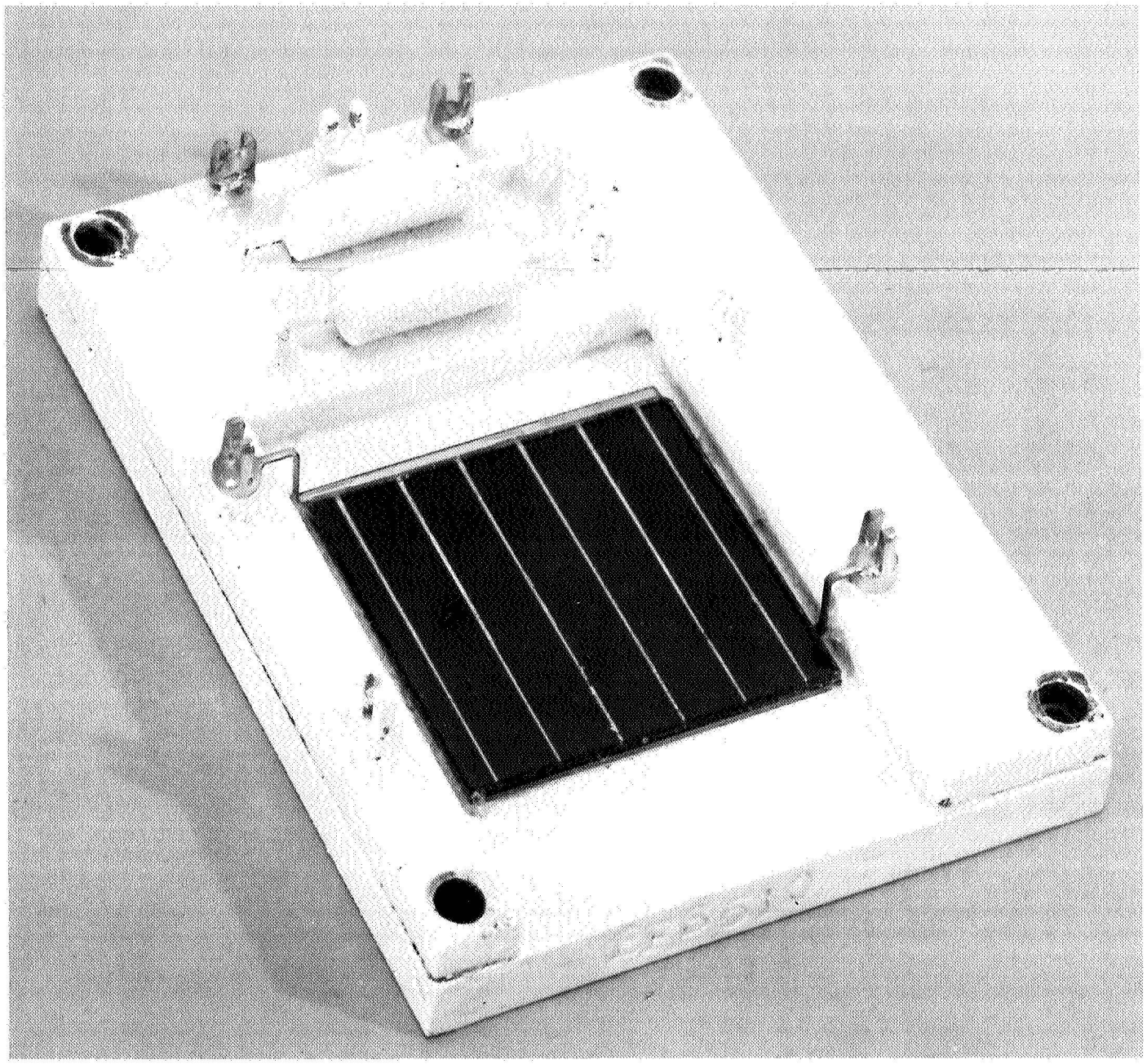

Fig. 3. *Mariner 1971* standard solar cell module

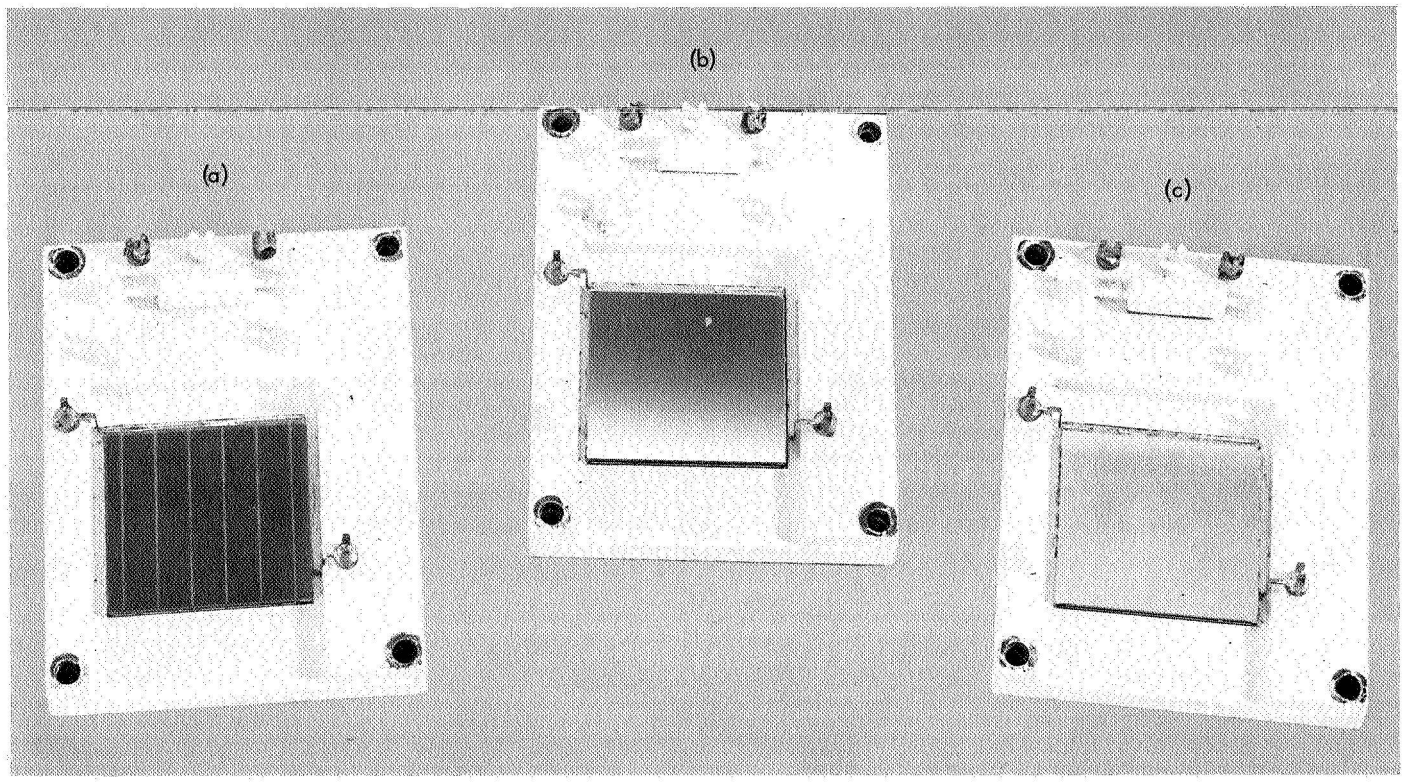

Fig. 4. Bandpass filters: (a) BFS-506, 0.41–0.55 μm, (b) BFS-507, 0.60–0.73 μm, (c) BFS-508, 0.70–0.82 μm

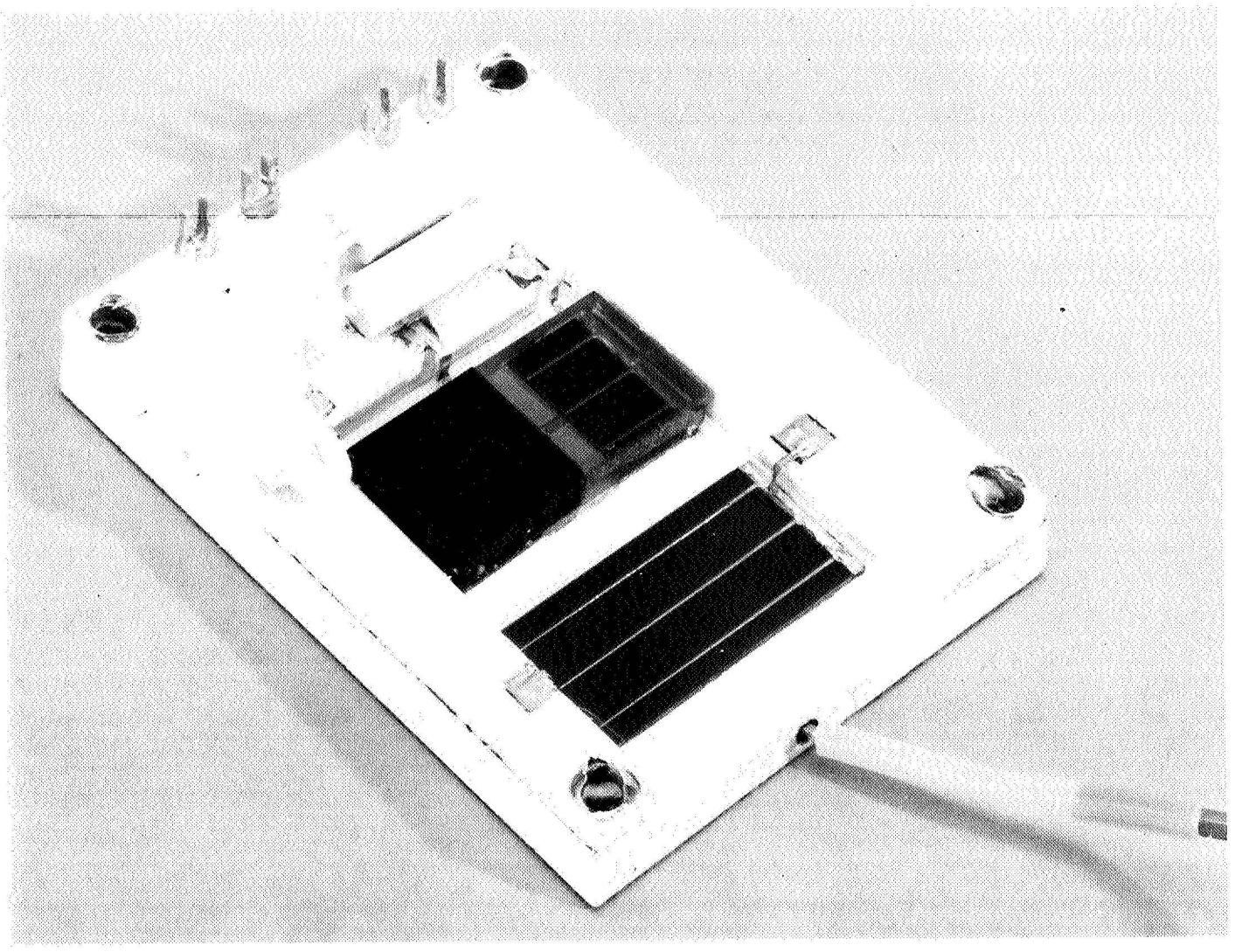

Fig. 5. Color ratio and intensity monitor

A chopper wheel was necessary to close off periodically all energy to the radiometers. This condition established a zero reference. A six-position filter wheel containing five long-wave-passing filters was placed directly below the chopper wheel. The sixth position was left open to permit a total radiation measurement. The chopper wheel and the filter wheel were advanced independently by separate geneva mechanisms triggered by the stepping switch. Figure 6 shows the complete radiometer experiment ready for flight.

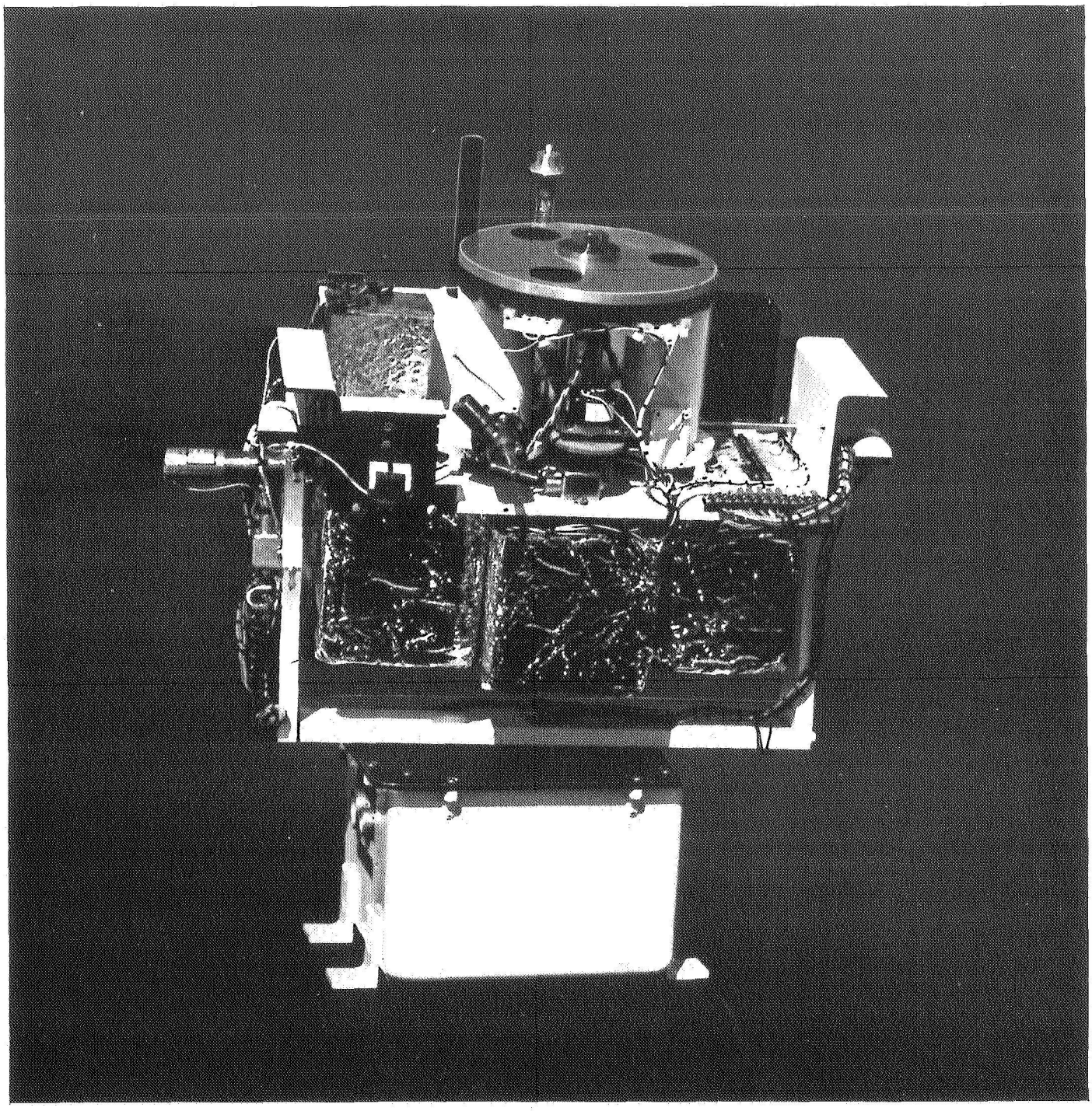

Fig. 6. Modified tracker for radiometer and filter wheel experiment

The filters employed are long-wave-passing interference filters deposited on water-free quartz material. The five filters have respective cut-on points (50% transmission) at 0.402, 0.589, 0.675, 0.772, and 0.835 μm, and the transmission of each filter extends to the limit of quartz, approximately 3.5 μm.

IV. Balloon Flight Performance

Flight 1 of the 1968 series was launched on July 19, 1968. The balloon reached a maximum altitude of 82,800 ft (25,237 m) and remained above the 80,000-ft mark throughout the 4-h float period, as shown by the time–altitude profile (Fig. 7). The modified tracker performed as expected, and good data were returned from the flight. No damage was inflicted to either the solar cells or solar tracker upon earth impact.

Flight 2 was launched 10 days later, on July 29, 1968. The balloon ascended normally and reached a float altitude of 82,800 ft (25,237 m) at 10:20 Central Daylight Time (CDT). After floating at this altitude for slightly over 1 h, the balloon began a gradual descent, passing through the 76,000-ft (23,165-m) mark at approximately 13:00 CDT. The balloon continued to lose altitude and was at 66,200 ft (20,178 m) when the descent valve was opened by a preset timer. The descent rate increased initially but slowed to less than 60 ft/min at a 40,000-ft (12,192-m) altitude. When the backup safety control unit actuated the balloon release squibs, causing the upper and lower payloads to separate, the balloon was still at 34,000 ft (10,363 m). (The backup unit is necessary to comply with Federal Aviation Agency regulations to clear the airlanes before sunset.) The lower payload descended via parachute and landed without damage. Due to the shock of the lower payload release, the balloon apparently ruptured, and the upper payload, along with the balloon material, essentially free-fell, impacting in a cornfield and inflicting extensive damage on the tracker. Two solar cell modules were slightly damaged; on one, a load resistor was broken, and on the other, the solar cell cover glass was chipped.

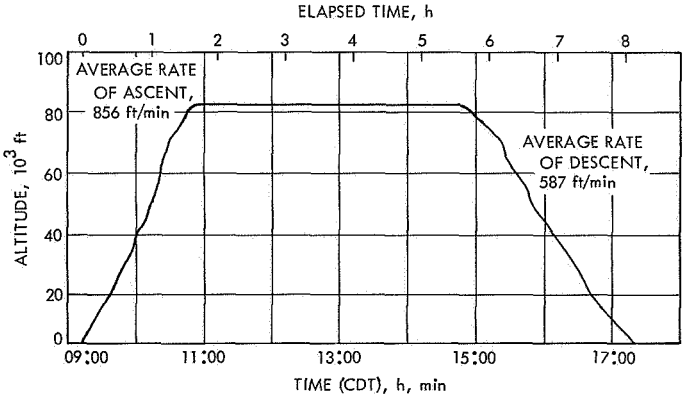

Fig. 7. Typical altitude profile for 80,000-ft flight. Balloon was launched on July 19, 1968, at 09:12 CDT, from the Litton Flight Facility, New Brighton, Minn.; surface wind, north at 3 mi/h. Impact was at 17:20 CDT, at Ellsworth, Wis.

The balloon's loss of altitude is attributed to a cloud layer that moved between the earth and the balloon after launch. The cloud layer reduced earth heat radiation reaching the balloon and upset the thermal equilibrium achieved during the early float period. As the day progressed, the cloud layer became heavier, further reducing the heat radiation from the earth, causing the helium gas to cool, and resulting in a loss of lift. When the descent valve (located on the side of the balloon) was opened, the helium had cooled and contracted to the point where an insufficient amount could be valved off to maintain balloon descent to the earth. The Litton final report (Ref. 2) gives a more detailed analysis of the balloon behavior during this flight.

Although the balloon did not remain above the desired altitude throughout the 4-h float period, good calibration data were recorded for more than 2 h.

Flight 3 was launched on August 20, 1968, after several consecutive days of bad weather. The top-mounted payload was some 11 lb (4.98 kg) heavier than the 54-lb (24.49-kg) payload normally flown, because of the weight of the special radiometer experiment. The added weight caused the top payload to sink deeply into the balloon material upon launch. The balloon ascended normally and performed perfectly through the flight. Average float altitude was 80,800 ft (24,628 m) during the 4-h float period.

Because of the cloud problem encountered on the previous flight, a ballast system was incorporated into the bottom payload for this flight. Four 7-lb (3.18-kg) bags of steel shot were suspended from the gondola, one bag tied to each of the four sides. The ballast system was operated by radio control from the flight center, and each bag could be commanded to open as required. Although cloud cover was not a problem on the third flight, the ballast was released during the float period to test the system and did provide effective altitude control.

Impact of the balloon was in a grove of trees in calm wind conditions. The recovery crew arrived at the site before the tracker had reached the ground and were able to recover the top payload without damage.

V. Discussion of Balloon Flight Data

A. Computer Data Reduction

A computer program written to handle the solar cell balloon data is used to convert the telemetry frequency data into millivolts. The computer further processes the data and corrects for intensity and temperature. Input to the computer is in the form of punched cards, supplied this year by the contractor. Data output is in two forms, digital printout and analog plots. The digital data become the standard cell calibrated values, whereas the analog data are useful to see the degree of scatter and the temperature profile. Figures 8 and 9 show a typical cell output and a typical temperature profile recorded during flight 1.

B. Flight 1 Data

Thirty data points were averaged for each of the standard solar cells on flight 1. The beginning time and ending time for data selection were chosen by an analysis of the analog temperature profile during the time the balloon was above 80,000 ft. (It is desirable to have a stabilized temperature during data recording. Best stabilized temperatures on flight 1 occurred between 12:08 and 15:11 CDT.)

The solar cell data corrected to 1 AU (139.6 mW/cm²) and to 28°C, along with pertinent solar cell and filter information, are tabulated in Table 1. The standard cell numbers identify the use of the standard, the cell manufacturer, or the cell type as follows:

OAO	Orbiting Astronomical Observatory Program
AEG	Allgemeine Elektricitäts-Gesellschaft
SIE	Siemens Aktiengesellschaft
BFS	Balloon Flight Standard (JPL designation)
LGY	NASA Langley Research Center
IPC	Ion Physics Corporation[2]
CDS	Cadmium Sulfide Cell Type
CDTE	Cadmium Telluride Cell Type
APL	Applied Physics Laboratory

[2]Burlington, Mass.

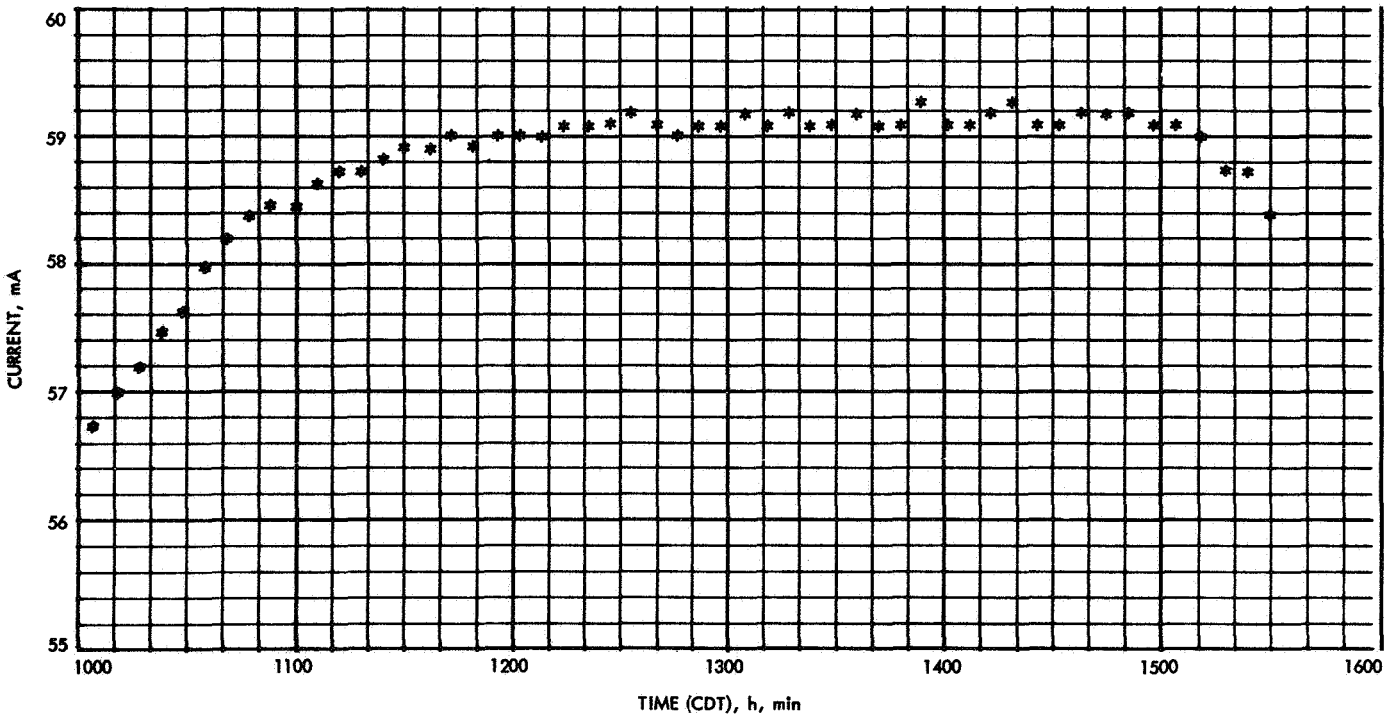

Fig. 8. Short-circuit current for BFS-17A, flight 1

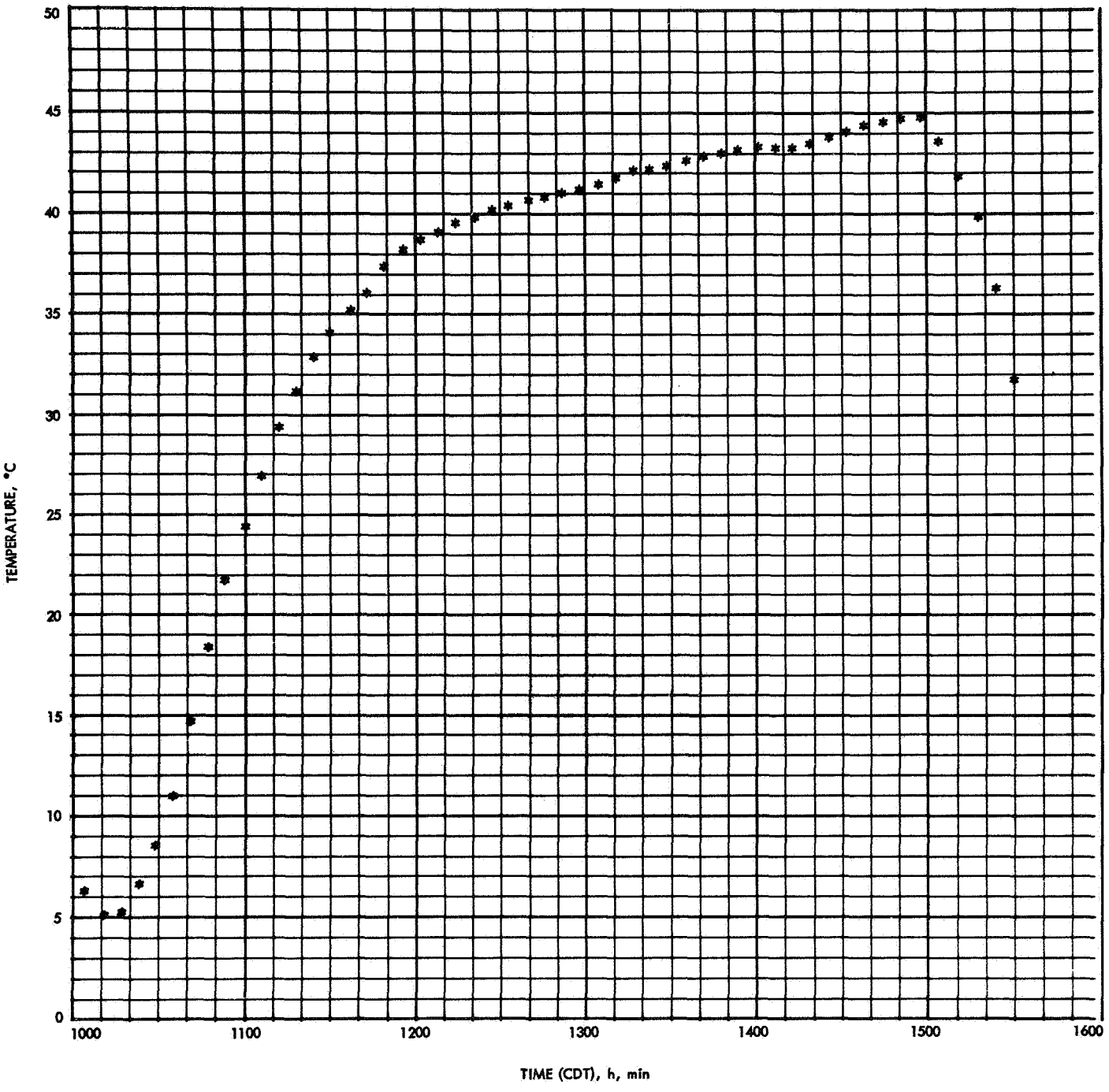

Fig. 9. Thermistor B2 temperature profile, flight 1

Table 1. Solar cell data, flight 1[a]

Standard cell number	Cell type	Cell size, cm	Cell load, Ω	Filter	Standard cell output, mV[b]
OAO-1A	*n–p*	1 × 2	1.0	0.41 μm cut-on	64.87
OAO-2A				0.41 μm cut-on	67.50
OAO-3A				0.41 μm cut-on	67.55
OAO-7B				None	67.86
AEG-19819		2 × 2	0.5		69.63
AEG-20004					70.00
SIE-129					73.58
SIE-139				0.41 μm cut-on	70.87
BFS-506			1.0	0.41–0.55 μm	31.29
BFS-507				0.60–0.73 μm	37.60
BFS-508				0.70–0.82 μm	30.00
BFS-17A	*p–n*	1 × 2		0.41 μm cut-on	60.31
BFS-17B	*p–n*	1 × 2			60.59
BFS-511	*n–p*	2 × 2	0.5		67.54
BFS-512			4.1		61.15
BFS-513			1.0 kΩ		57.90
BFS-514			0.5		68.45
LGY-168A		1 × 2	1.0	None	66.36
LGY-168B		1 × 2	1.0	None	66.75
IPC-1		2 × 2	0.5	0.40 μm cut-on	71.59
CDS-008A	CdS	1 × 2	1.0	Kapton	33.11
CDS-008B					33.62
CDS-009A					33.71
CDS-009B					33.49
CDTE-1A	CdTe			None	30.12
CDTE-1B	CdTe			None	29.50

[a]Flight date, July 19, 1968; altitude, 82,000 ft.
[b]Corrected to 139.6 mW/cm² and 28°C.

Table 2. Solar cell data, flight 2[a]

Standard cell number	Cell type	Cell size, cm	Cell load, Ω	Filter	Standard cell output, mV[b]
OAO-4A	*n–p*	1 × 2	1.0	0.41 μm cut-on	66.27
OAO-5A					67.28
OAO-6A					67.40
OAO-8B					67.22
AEG-20308		2 × 2	0.5	None	70.35
IPC-3		2 × 2	0.5	0.41 μm cut-on	70.60
SIE-134		2 × 2	0.5	None	74.66
APL-I		1 × 2	18.0	0.375–0.585 μm	82.31
BFS-516A	*p–n*	0.6 × 1	4.0	"Red" bandpass	25.30
BFS-516B		0.6 × 1	4.0	"Blue" bandpass	23.00
BFS-516C		1 × 2	1.0	0.41 μm cut-on	63.95
BFS-17A			1.0	0.41 μm cut-on	60.20
BFS-17B			1.0	0.41 μm cut-on	60.45
APL-II	*n–p*		18.0	0.585–0.700 μm	73.34
APL-III			20.0	0.700–0.830 μm	76.70
APL-IV			12.0	0.830–1.100 μm	72.13
APL-V			4.0	Quartz cover	79.11
LGY-268A			1.0	None	69.16
LGY-268B			1.0	None	67.25
IPC-2		2 × 2	0.5	0.41 μm cut-on	71.17
BFS-509		2 × 2	0.5	0.41 μm cut-on	66.99
BFS-510		2 × 2	0.5	0.41 μm cut-on	65.90
CDS-010A	CdS	1 × 2	1.0	Kapton	34.77
CDS-010B	CdS			Kapton	32.67
CDTE-2A	CdTe			None	35.09
CDTE-2B	CdTe			None	32.73

[a]Flight date, July 29, 1968; altitude, 80,000 ft.
[b]Corrected to 139.6 mW/cm² and 28°C.

C. Flight 2 Data

Although flight 2 was plagued with the altitude problem described above, 23 data points were recorded during the 2-h period the balloon was above 76,000 ft. The average stabilized temperature above the 76,000-ft altitude was 42.5°C and was recorded between 11:16 and 13:38 CDT.

The corrected solar cell data and cell description for flight 2 are given in Table 2.

D. Flight 3 Data

Because of the special circuitry and the filter wheel assembly, data recorded on flight 3 were only partially reduced by computer. The data stepping switch time was increased from 10 to 20 s to allow for the slower response time of the radiometers. This condition gave a total of 18 data points at a stabilized temperature during the float period. Since the 6-position filter wheel advanced one position for each 36-channel data cycle, only three data points were recorded for each cell–filter combination. The averages of the three data points, corrected for filter

transmission loss but uncorrected for intensity and temperature, are listed in Table 3. The short-circuit current in a particular energy band was determined by finding the difference between readings of spectrally adjacent filters. The solar cell filter wheel experiment presents data that give an indication of the combined spectral response of the solar cell and the spectral distribution of space sunlight. Figure 10 shows in graphic form the combined response of the four different solar cells in the experiment. Since these curves were constructed using only four data points, they can only serve to indicate the peak spectral response of the solar cell under space sunlight.

Probably the most significant single accomplishment of the solar cell standardization program in 1968 was the measurement of the solar constant using the active cavity radiometers. The measurement of the solar constant by balloon-borne radiometers represents the first time a direct measurement has been made in which the effects of the earth's atmosphere were not the limiting source of experimental uncertainty. The value of the solar constant thus determined, which may be put forth as the most accurate presently available, is

$$139.0 \pm 0.9 \text{ mW/cm}^2 \qquad \text{(Ref. 3)}$$

The presently accepted solar constant value of 139.6 $\pm$2.8 mW/cm^2 was established by Johnson in 1954 (Ref. 4). A technical report presenting the details of the radiometer design and experimental results is being prepared by the Instrumentation Section of the Jet Propulsion Laboratory.

E. Postflight Simulator Correlation Measurements

Following the balloon flight calibration, all standard solar cells were returned to JPL and measured in the X-25L solar simulator. The purpose of the measurements

Table 3. Balloon flight filter wheel experiment[a]

Standard cell number[b]	Flight data for indicated discrete energy band						Total short-circuit current, mA
	<0.402 μm	0.402–0.589 μm	0.589–0.675 μm	0.675–0.772 μm	0.772–0.835 μm	>0.835 μm	
	Short-circuit current, mA						
BFS-501	0.94	32.38	25.22	25.96	8.60	41.02	134.12
BFS-502	0.24	26.32	23.52	24.94	8.14	34.88	118.04
BFS-503	0.00	31.26	25.04	24.96	8.34	43.38	132.98
BFS-504	1.26	38.08	24.28	23.84	8.28	29.04	124.78
	% of short-circuit current						
BFS-501	0.70	24.14	18.80	19.36	6.41	30.58	
BFS-502	0.20	22.30	19.93	21.13	6.90	29.55	
BFS-503	0.00	23.51	18.83	18.77	6.27	32.62	
BFS-504	1.01	30.52	19.46	19.11	6.64	23.27	
	Short-circuit current per unit wavelength, mA/nm						
BFS-501	—	0.173	0.293	0.268	0.137	—	
BFS-502	—	0.141	0.273	0.257	0.129	—	
BFS-503	—	0.167	0.291	0.257	0.132	—	
BFS-504	—	0.204	0.282	0.246	0.131	—	

[a]Flight date: Aug. 20, 1968; altitude: 80,800 ft; average float temperature: 36.5°C; calculated intensity from 1968 ephemeris tables (ref. 139.6 mW/cm^2 average intensity): 136.4 mW/cm^2; measured intensity from radiometer experiment: 135.8 mW/cm^2.

[b]Solar cell description:

BFS-501 Heliotek, 2 × 2 cm × 0.018 in. (0.457 mm), *n–p*, 1–3 Ω-cm (*Mariner 1969* type)

BFS-502 Heliotek, 2 × 2 cm × 0.008 in. (0.2032 mm), *n–p*, 1–3 Ω-cm

BFS-503 Ion Physics Corp., 2 × 2 cm × 0.018 in., *n–p*, 10 Ω-cm (ion-implanted silicon)

BFS-504 Texas Instruments, Inc., Dallas, Tex., 2 × 2 cm × 0.004 in. (0.1016 mm), *n–p*, 1–3 Ω-cm

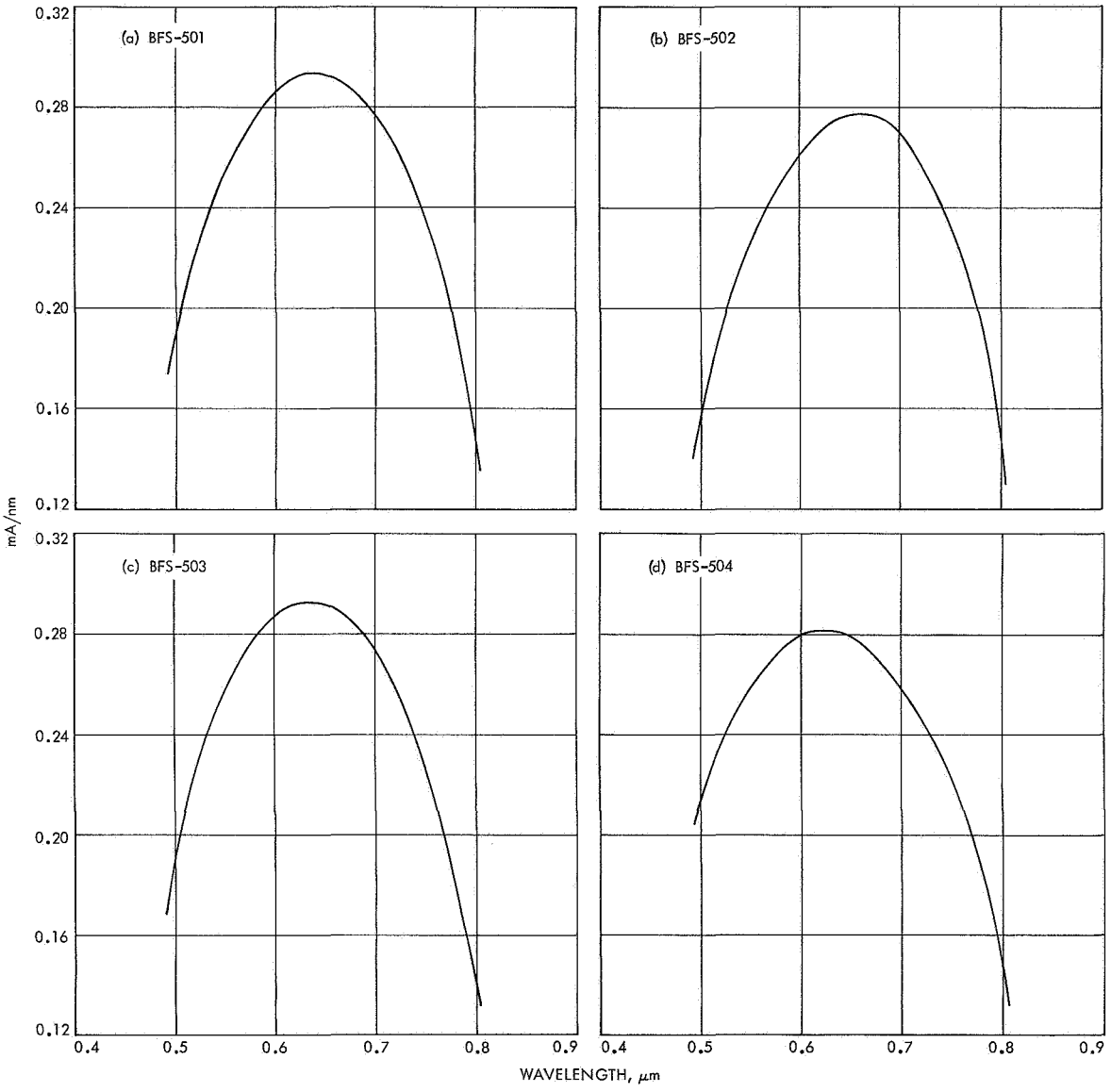

Fig. 10. Response of four solar cells in filter wheel experiment

was to ensure that the standard cells were undamaged because of earth impact or handling and transportation. The intensity of the simulator was adjusted to a zero air mass sunlight equivalent of 139.6 mW/cm², using a previously flown balloon standard, BFS-17A. Temperature of the cells was maintained at 28 ±1°C.

The results of the correlation measurements confirm the necessity of using a standard solar cell that is representative of the cells or solar array under test. Cell types other than silicon or silicon cells covered with spectrally selective filters showed deviations from the balloon calibration of nearly 10%, as listed in Table 4. The deviation is due to the fact that even closely filtered simulators, such as the X-25L, do not exactly duplicate the sun's spectrum even in the spectral response region of a solar cell. However, by selecting a representative standard solar cell, zero air mass measurements to better than 1% can be made in the X-25L solar simulator.

F. Analysis of Temperature Coefficients

The present balloon flight payload configuration reaches a temperature stabilization point of approximately 40°C at float altitude. Since the short-circuit current of a silicon solar cell increases as the temperature increases, corrections must be made to the calibrated cell output to operate the cell at a standard temperature of 28°C. As the balloon ascends through the troposphere, solar cell temperatures lower and approach 0°C. By the time the balloon reaches float altitude, the solar cells have not reached a stabilized temperature, due to the thermal lag associated with the copper substrate on which the cell is mounted and also with the aluminum plate on which the copper substrate is mounted.

Figure 9 shows the temperature of the solar cell payload plotted as a function of time. From 10:50 until 14:50, the balloon was at its float altitude. During this same time period, the solar cell temperature increased from 20 to 44.7°C. By plotting the short-circuit current of a solar cell as a function of temperature while the cell is under stable intensity conditions, the temperature coefficient α of the cell can be determined. Figure 11 is an example of the temperature coefficient of a 1 × 2-cm, *p–n*, 2-Ω-cm cell determined by this method. Accuracy is limited because of the nonsimultaneous readings of short-circuit current and temperature when the temperature is increasing rapidly during the early portion of the float period. As the temperature begins to stabilize, more accurate data can be obtained.

Table 4. Sampling of cell types flown on the 1968 balloon flights

Standard cell number	Balloon calibration value, mV[a]	X-25L simulator calibration value, mV[b]	Deviation from balloon calibration, %
OAO-1A	64.87	64.3	−0.88
OAO-4A	66.27	66.6	+0.50
LGY-168A	66.36	65.8	−0.84
IPC-1	71.59	70.6	−1.38
CDS-008A	33.11	33.7	+1.78
CdTe-1A	30.12	27.2	−9.69
SIE-129	73.58	73.1	−0.65
AEG-20004	70.00	69.5	−0.71
BFS-510	65.90	65.8	−0.15
BFS-514	68.45	67.5	−1.39
BFS-506	31.29	31.4	+0.35
BFS-507	37.60	40.0	+6.38
BFS-508	30.00	31.4	+4.67
BFS-516A	25.30	23.8	−5.93
BFS-516B	23.00	22.1	−3.91
BFS-516C	63.95	63.0	−1.49

[a]Corrected to 139.6 mW/cm² and 28°C.

[b]At 139.6 mW/cm² and 28°C. The simulator intensity was set using the balloon standard BFS-17A (Heliotek 1 × 2 cm, *p–n*, 2 Ω-cm cell with a 0.410-μm filter made by the Optical Coating Laboratory, Inc., Santa Rosa, Calif.)

The temperature coefficient values of silicon solar cells obtained from the method described agree well with laboratory X-25L experimental results for bare cells or cells with a normal 0.41-μm cut-on filter. It was noted that cells with optical bandpass filters flown on the 1968 balloon series exhibited a pronounced difference in the short-circuit current temperature coefficient compared with

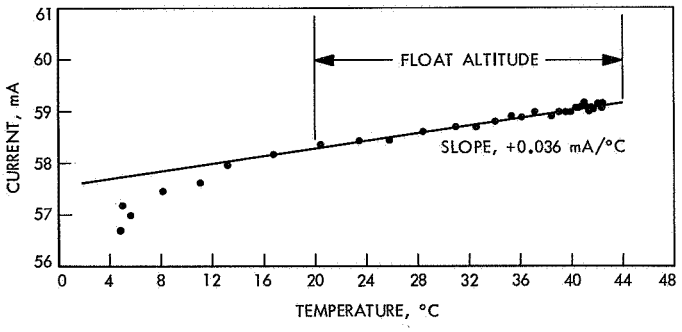

Fig. 11. Temperature coefficient for cell BFS-17A, determined from the short-circuit current

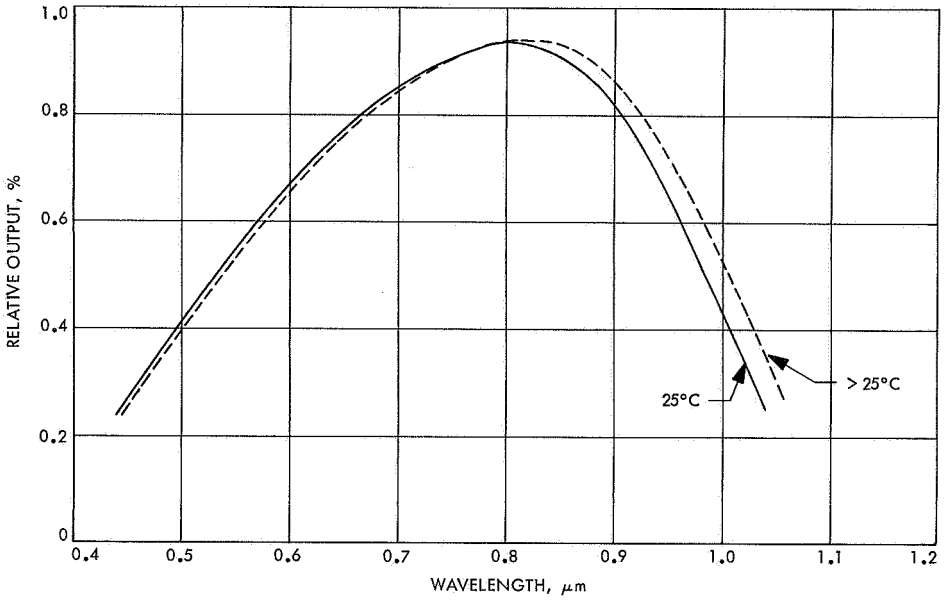

Fig. 12. Solar cell spectral response, showing temperature dependence

similar unfiltered cells. This can be expected since a difference in temperature coefficients has been observed between cell measurements under light sources of different spectral distribution, i.e., tungsten light, terrestrial sunlight, and filtered xenon light. Therefore, when a filter is placed over a solar cell, the spectral distribution to that cell is effectively changed, depending upon the cut-on and cut-off points of the filter.

Laboratory measurements have shown that the spectral response of a silicon solar cell is temperature-dependent; that is, with increasing temperature, the entire response curve shifts toward the infrared. However, the ultraviolet response does not shift nearly as much as the infrared response (Fig. 12). A silicon solar cell covered by a filter having a bandpass of, say, 0.4 to 0.5 μm will exhibit a negative temperature coefficient, since, with an increase in temperature, there is a corresponding decrease in short-circuit current. By the progressive replacement of this filter with successive filters of 0.1-μm band widths continuing from 0.5 to 1.2 μm, the temperature coefficient will decrease to zero and then go positive as the longer wavelengths are reached, where an increase in temperature produces a corresponding increase in short-circuit current. Figure 13 shows the temperature dependence of the short-circuit current for three similar solar cells, each covered with a filter having a different bandpass.

From this analysis, it can be seen that a similar effect will result if a cell–filter combination such as BFS-508

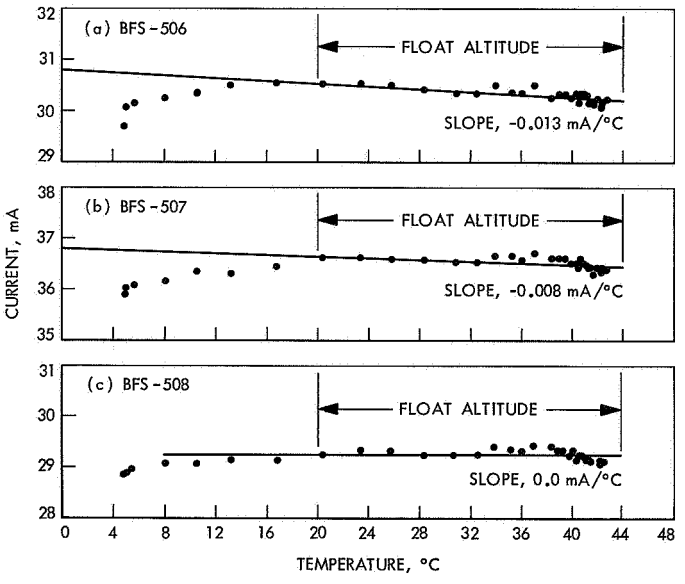

Fig. 13. Short-circuit current vs temperature for three solar cells

(Table 5) is monitored as the temperature increases from room temperature. Initially, the temperature coefficient will be positive; it will then go negative as the spectral response curve of the solar cell shifts toward the infrared with increasing temperature. The beginning of this effect is evident in Fig. 13 toward the higher temperatures. Therefore, it can be seen that the short-circuit current temperature coefficient is subject to the solar cell spec-

tral response as well as the illuminating source spectral distribution.

The temperature coefficients given in Table 5 were determined by the method described above for the JPL solar cells on the first two balloon flights of the 1968 series.

VI. Future Plans

To keep abreast of solar cell development efforts, it is planned to conduct high-altitude balloon flights on a regularly scheduled basis to provide applicable standard solar cells for a variety of space projects. In addition to providing standard cells, a method of measuring the solar constant has been established, and additional flights with improved detection instruments are planned. Concentrated work in this area could permit a measurement of the sun's energy as a function of wavelength by flying a compact spectrophotometer above the earth's atmosphere.

Table 5. Temperature coefficients

Standard cell number[a]	Load, Ω	Filter description	Temperature coefficient, mA/°C
BFS-506	1.0	0.41- to 0.55-μm bandpass Corning 7940 fused silica	−0.013
BFS-507	1.0	0.60- to 0.73-μm bandpass Corning 7940 fused silica	−0.008
BFS-508	1.0	0.70- to 0.82-μm bandpass Corning 7940 fused silica	0.0
BFS-509[b]	0.5	0.41-μm cut-on 20-mil Corning 7940 fused silica	+0.128
BFS-510[b]	0.5	↓	+0.143
BFS-511	0.5	↓	+0.104
BFS-512	4.09	↓	−0.173 mV/°C
BFS-513	1 kΩ	↓	−2.23 mV/°C
BFS-514	0.5	↓	+0.102
BFS-516A[b]	4.0	Corning No. 7-69 "Red" bandpass	−0.006
BFS-516B[b]	4.0	Corning No. 1-57 "Blue" bandpass	−0.018
BFS-516C[b]	1.0	0.41-μm cut-on 6-mil Corning 0211 Microsheet	+0.023
BFS-17A	↓	↓	+0.036
BFS-17A[b]	↓	↓	+0.036
BFS-17B	↓	↓	+0.040
BFS-17B[b]	↓	↓	+0.039

[a]BFS-506–BFS-514 use Heliotek 2 × 2-cm × 0.018-in., *n–p*, 2-Ω-cm cells (*Mariner 1969* type).

BFS-516C and BFS-17A and B use Heliotek 1 × 2-cm × 0.018-in., *p–n*, 2 Ω-cm cells.

BFS-516A, B use the same cell type as BFS-516C except that the size is 0.6 × 1 cm.

All filters are of the interference type except BFS-516A and B, which are of the absorption type.

[b]Flight No. 2. All other data are from flight 1.

VII. Summary

The data presented in this report provide additional confidence in the balloon flight calibration technique. In Table 6, the measurements of one standard silicon *p–n* solar cell flown as a reference over a 6-yr period show repeatability to be within 1%. The data also show that silicon solar cells are reliable for standards over a long term if handled properly. Refinements in measurement technique and system stability have been incorporated through the years to increase system accuracy and repro-

Table 6. Repeatability of standard solar cell BFS-17A for 16 flights over a 6-yr period[a]

Flight date	Deviation from mean, %	Output, mA
Sept. 5, 1963		60.07
Aug. 3, 1964		60.43
Aug. 8, 1964		60.17
July 28, 1965		59.90
Aug. 9, 1965		59.90
Aug. 13, 1965		59.93
July 29, 1966		60.67
Aug. 4, 1966		60.25
Aug. 12, 1966		60.15
Aug. 26, 1966		60.02
July 14, 1967		60.06
July 25, 1967		60.02
Aug. 4, 1967		59.83
Aug. 10, 1967		60.02
July 19, 1968		60.31
July 29, 1968		60.20
Mean output	Maximum, 0.92 Rms, 0.35	60.12

[a]Each data point is an average of 20–30 data points from each flight. All data are normalized to 139.6 mW/cm² and to a cell temperature of 28°C.

ducibility. Standard solar cells calibrated by means of balloon flights are maintained for use with JPL flight programs. The cooperative effort program has proved very useful in providing standard solar cells to other government agencies. As new solar cell types are developed and are used in fabricating solar arrays, standard solar cells of the new type are required to assist in establishing the array performance characteristics.

The flexibility of the balloon flight system has been demonstrated by adapting radiometers to the solar tracker in place of solar cells. As a result of this experiment, a more accurate measurement of the solar constant was made.

The use of high-altitude balloons has proved to be a feasible, reliable, and economical method of obtaining standard solar cells.

References

1. Kendall, J. M., Sr., *The JPL Standard Total-Radiation Absolute Radiometer*, Technical Report 32-1263. Jet Propulsion Laboratory, Pasadena, Calif., May 15, 1968.
2. Conlon, R. D., *Solar Tracker Balloon Flights 3048, 3049, and 3050*, Report 3269, JPL Contract 952223. Applied Science Division, Litton Systems, Inc., Nov. 1968.
3. Willson, Richard C., *An Experimental and Theoretical Comparison of the JPL Radiometric Scale and the International Pyrheliometric Scale*, Technical Report 32-1365. Jet Propulsion Laboratory, Pasadena, Calif., Feb. 1, 1969.
4. Johnson, F. S., "The Solar Constant," *J. Meteorol.*, Vol. 11, p. 431, Dec. 1954.